Comparing a Regional, Subcontinental, and Long-Range Lightning Location System over the Benelux and France

DIETER R. POELMAN

Royal Meteorological Institute, Brussels, Belgium

FRANÇOISE HONORÉ

Météo-France, Toulouse, France

GRAEME ANDERSON

Met Office, Exeter, United Kingdom

STÉPHANE PEDEBOY

Météorage, Pau, France

(Manuscript received 26 November 2012, in final form 3 June 2013)

ABSTRACT

Increasing possibilities for using lightning data—for instance, in monitoring and tracking applications—necessitate proper spatial and temporal mapping of lightning events. It is therefore of importance to assess the capabilities and limitations of a ground-based lightning network of interest to locate electromagnetic signals emitted by lightning discharges. In this paper, data covering two storm seasons, between May and September 2011 and 2012, are used to compare the spatial and temporal lightning observations of three different lightning location systems over an area covering the Benelux and France. The lightning datasets from a regional network employing Surveillance et Alerte Foudre par Interférométrie Radioélectrique (SAFIR) sensors operated by the Royal Meteorological Institute of Belgium (RMIB), a subcontinental network operated by Météorage (MTRG), and the Met Office's long-range Arrival Time Difference network (ATDnet) are considered. It is found that the median location difference among corresponding strokes and flashes between ATDnet and MTRG is 1.9 and 2.8 km, respectively, and increases by a factor of ~3 when comparing ATDnet and/or MTRG to SAFIR. The absolute mean time difference between shared events fluctuates between approximately 25 and 100 μs. Furthermore, lightning data are correlated in terms of relative detection efficiency, quantifying the number of detections that coincide between two different networks. The highest relative values are found among ATDnet and MTRG. In addition, a lower limit of ~25% of ATDnet's flashes are of type inter/intracloud. Finally, it is demonstrated that all three networks are competent in mapping the electrical activity in thunderstorms.

1. Introduction

Numerous lightning location systems (LLS) exist to date employing a variety of sensors and detection techniques, operating at very low/low frequencies (VLF/LF) up to the very high frequencies (VHF). An LLS employs either sensors of a single type or a combination of different sensors. Depending on the type of operating sensors, angle and/or timing information is provided. This, in turn, determines whether a (magnetic) direction finding (MDF) technique, a time-of-arrival (TOA) technique, or a combination is used by the central processor to retrieve unambiguous solutions from the raw data.

The different national meteorological services (NMS) in Europe obtain lightning data via two different routes: either provided by their own networks or purchased from the available commercial providers. This diversity makes it challenging to interchange information among each other. However, with the ongoing evolution of

Corresponding author address: Dieter R. Poelman, Royal Meteorological Institute, Ringlaan 3 Avenue Circulaire, B-1180 Brussels, Belgium.
E-mail: dieter.poelman@meteo.be

DOI: 10.1175/JTECH-D-12-00263.1

lightning detection possibilities, lightning data plays an ever-increasing role in, for instance, real-time storm monitoring and leads to the development of specific applications, such as automated storm tracking and nowcasting (Kohn et al. 2011).

Several techniques can be employed to investigate the performance of a network in terms of its detection efficiency (DE); location accuracy (LA); peak current estimate; and classification of the observed lightning type, that is, negative versus positive and/or cloud-to-ground (CG) versus cloud-to-cloud (CC) signals. The most desirable way to do this is by using so-called ground-truth data. The latter can be gathered from direct hits to towers (Diendorfer 2010), measurements of rocket-triggered lightning (Jerauld et al. 2005; Nag et al. 2011), or via video and electric field (E-field) measurements (Biagi et al. 2007; Schulz et al. 2010; Poelman et al. 2013). However, ground-truth observations are not readily available at all times.

Another way to test a lightning network is through the use of satellite data. Several studies have tried to correlate detections from ground-based LLS to observations from satellite-based optical lightning detectors, that is, the Optical Transient Detector (OTD) and Lightning Imaging Sensor (LIS) (Boccippio et al. 2000; Thomas et al. 2000). These studies have shown promising results correlating the observed flashes. However, focus has been more on the ability of the satellite instruments to detect different types of lightning. With the launch of the next generation of satellites with state-of-the-art instruments, such as the Lightning Imager (LI) on board the Meteosat Third Generation (MTG) geostationary satellite, observations from space are to become more continuous, homogeneous, and reliable. Nonetheless, the spatial accuracy is expected to be lower than ground-based LLS.

Intercomparison studies between LLS within regions of overlapping coverage offer an additional way to analyze detections made by one network in comparison to another. The best way is to monitor the behavior over an extended period, spanning several thunderstorm seasons in order to remove potential biases due to, for example, sensor outages. Care must be taken to interpret the outcome, as different networks make use of different processing algorithms and are unlikely to have similar detection efficiencies. Nevertheless, such studies can contribute to a more thorough understanding of the performance of a particular LLS. Examples of some of these studies include correlating detections made by the World Wide Lightning Location Network (WWLLN) to local networks (Jacobson et al. 2006; Rodger et al. 2006; Abreu et al. 2010), comparing CG flash observations between the Korea Aerospace Research Institute Total Lightning Detection System (KARITLDS) and the Korean Meteorology Administration Lightning Detection Network (KLDN) in South Korea (Kuk et al. 2011), correlating data from the experimental network National Observatory of Athens (ZEUS) against the lightning detection network (LINET) over western Europe (Kotroni and Lagouvardos 2008; Lagouvardos et al. 2009), and comparing a regional network based on Surveillance et Alerte Foudre par Interférométrie Radioélectrique (SAFIR) sensors against the operational German network Blitz Informationsdienst von Siemens (BLIDS; Drüe et al. 2007). These have proven to be valuable for the interpretation of the detections made by the ground-based lightning networks.

In this paper, lightning data from the NMS of Belgium, France, and the United Kingdom are cross correlated. A description of the different networks is found in section 2. Section 3 describes the data and methodology used for comparison purposes. In sections 4 and 5, we compare the different networks over an area covering Belgium and an extended region, respectively. We conclude and summarize in section 6.

2. Networks

a. Météorage

The French national lightning location system has been operated by Météorage (MTRG) since 1986. It detects low-frequency electromagnetic signals generated by CG lightning, as well as a fraction of large-amplitude CC discharges. In the beginning, the LLS was made up of sensors placed only in France. Over the years this core network expanded with compatible sensors of neighboring partners, providing seamless extended observation coverage over western Europe. Currently, data from the different sensors are processed simultaneously using Vaisala's Total Lightning Processor (TLP) set in the operational centers of Météorage and Météo-France in Pau and Toulouse, respectively. At the time of this study, the lightning location system is made up of a mix of different sensors, as seen in Fig. 1, such as Improved Performance from Combined Technology (IMPACT) and Lightning Position and Tracking System (LPATS) sensors. Additionally, the French, German, and Austrian sensors are of type LS7001, operating the latest so-called onset time correction (Honma et al. 2011). This onset time correction aims at improving the arrival time estimate through a higher sampling of the waveform at the sensor. As such, improved location accuracy is expected in regions employing LS7001 sensors (Cummins et al. 2011; Honma et al. 2011). Since Spain, Italy, and the United Kingdom are covered by the

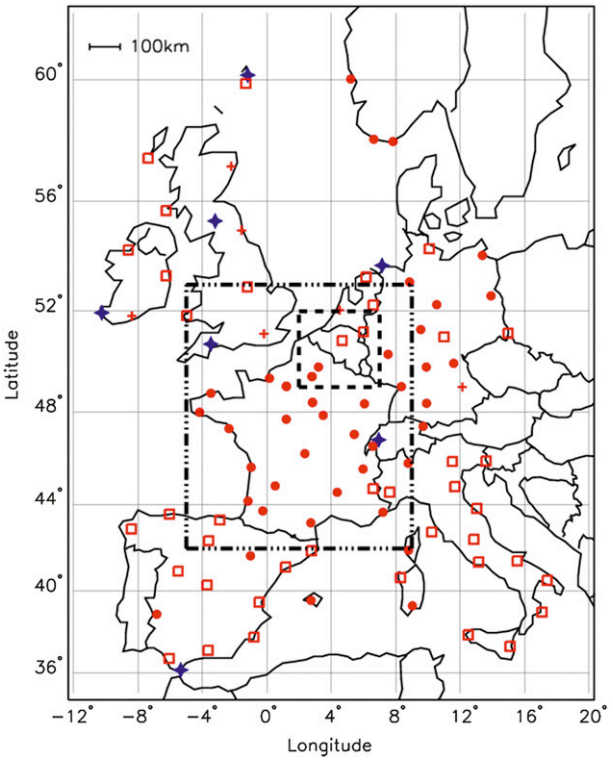

FIG. 1. Sensor positions for MTRG are plotted in red with IMPACT (open square), LPATS (plus sign), and LS7001 (filled circle) sensors. In addition, some sensors of ATDnet are plotted (blue stars). The two research areas are indicated as well. Dashed lines depict research area 1, whereas dashed–dotted lines outline research area 2.

older IMPACT and LPATS sensor models, the latter areas do not exhibit the same performance in terms of CG and CC detections compared to the regions exploiting LS7001. Hence, such a patchwork of different types of sensors and maintenance policies leads to an inhomogeneous quality of lightning detection over the network's coverage.

Depending on the region of interest, median LA values ranging from 440 to 600 m and a stroke and flash DE of about 85% and 100%, respectively, are found based on video records (Schulz et al. 2010; Poelman et al. 2013).

In what follows, we denote with MTRG the dataset containing solely CG detections, whereas MTRG$^+$ is used as an extended dataset containing CG, as well as the observed large-amplitude CC discharges due to the LS7001 capability. The discrimination between CC and CG discharges is based on predefined peak-to-zero threshold values. Overall, the amount of cloud pulses observed by this network equals the number of detected CG discharges, but areas with small baselines between LS7001 sensors exhibit increased CC detections, as further discussed in section 5a.

b. *Met Office*

The Met Office (UKMO) owns and operates a long-range lightning location network called the Arrival Time Difference network (ATDnet). The network has been in continuous operation since its initiation in 1987 and has undergone significant expansion and development in recent years, with the network currently consisting of 18 sensors deployed across Europe, Africa, the Indian Ocean, and the Caribbean and Asia. Eleven of these sensors are currently used for operational processing, giving good coverage over all of Europe. The seven additional sensors are positioned farther afield and are intended to provide improved long-range coverage in the near future, but have not as yet been integrated into the operational network. The network exploits VLF radio pulses emitted by lightning, locating the sources by measuring the time of arrival when the peak energy of the emitted waveform arrives at each sensor site. As VLF signals propagate over thousands of kilometers with low attenuation, ATDnet can locate lightning over 10 000 km from the network center in northwest Europe.

Performance estimates are calculated over the United Kingdom and Europe with a stroke DE of up to 90% and a median LA of ~2–3 km (Keogh et al. 2006). However, recent performance measurements, based on ground-truth data over Belgium (Poelman et al. 2013) indicate a stroke DE of 58%, a flash DE of 88%, and a median random location uncertainty of 1 km. Additionally, it is important to note that ATDnet's performance is subject to interference between different modes of ionospheric VLF reflections and diurnal changes of the ionospheric height (Bennett et al. 2010, 2011). The locations of the sensors in western Europe are plotted in Fig. 1.

c. *Royal Meteorological Institute of Belgium*

The Royal Meteorological Institute of Belgium (RMIB) has been operating an LLS since 1992. This network consists of four sensors of type SAFIR, with baselines ranging from 100 up to 180 km; see Fig. 2. The central processor uses an interferometric lightning location retrieval method in the VHF band to retrieve the location of intracloud source points using triangulation. In addition, the sensors are equipped with an E-field antenna detecting the LF return stroke signature, allowing the system to discriminate between CC and CG electrical signals on the basis of the rise and decay times of the observed waveform. Once an LF signal is detected, the CG stroke is assigned a location using the position of a time-correlated VHF signal. A minimum of two sensors are required to pick up the electromagnetic radiation

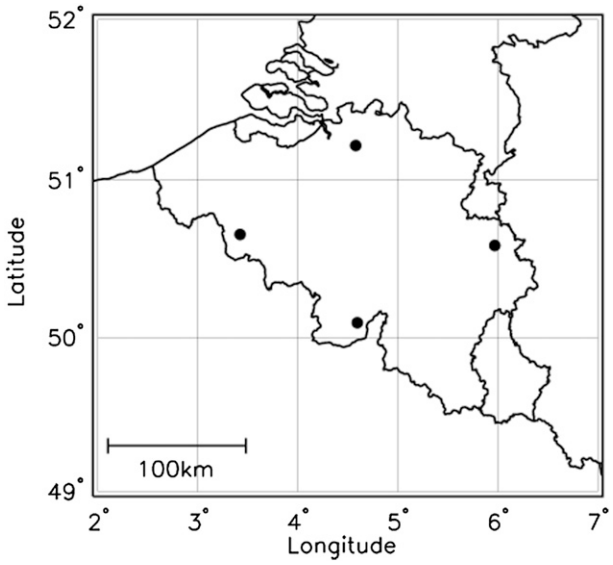

FIG. 2. Location of the four SAFIR sensors (dots) within the network operated by RMIB.

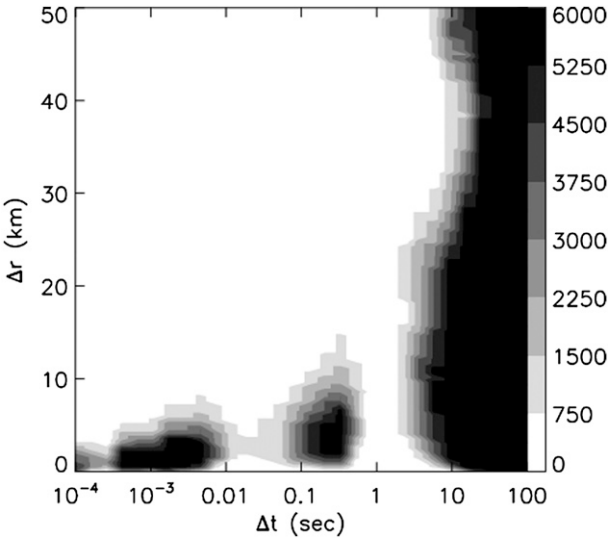

FIG. 3. Single-point signal autocorrelation plot, visualizing the temporal and spatial correlation among lightning detections observed by the total lightning SAFIR network of RMIB during a typical storm day. Gray shades indicate the number of signals per area, adopting a bin size of $10^{0.2}$ for Δt and 0.5 km for Δr.

from the same discharge. Even though the SAFIR network is a total lightning network, locating both VHF and LF signals, we solely use in the course of this paper the LF part of the SAFIR data for the intercomparison, in order to compare signals from corresponding processes in the formation of a discharge w.r.t. the other VLF/LF networks.

The performance of SAFIR has been tested recently against ground-truth data using video and E-field measurements (Poelman et al. 2013), resulting in a median LA of 6 km and a stroke and flash DE of 70% and 93%, respectively, in Belgium.

3. Data and methodology

Stroke data between May and September 2011 and 2012 are used for the analysis. Even though positive strokes with small peak currents (<10 kA) are likely to be misclassified as CG discharges when in fact those are more likely to be of intracloud nature (Cummins et al. 1998; Wacker and Orville 1999a,b; Jerauld et al. 2005; Orville et al. 2002; Cummins et al. 2006; Biagi et al. 2007; Grant et al. 2012), we opt not to remove them, as the goal of this study is to compare the operational datasets. Note that positive strokes with peak currents smaller than 10 kA contribute only by 1.5% and 4% to the dataset of SAFIR and MTRG, respectively. Hence, its influence on the results is minimal. Besides, ATDnet does not provide peak current estimates. Thus, removal of those positive strokes would induce an unequal treatment of the SAFIR and MTRG data compared to ATDnet.

When comparing flashes from different lightning networks, it is a necessity to have a common definition of a flash. Therefore, strokes located by the different networks are grouped into flashes in the same manner to yield compatible flash data as follows. Applying the methodology presented in Finke (1999) and Drüe et al. (2007) to the total lightning dataset (LF and VHF) of SAFIR, one can group single-point signals according to their separation in time and space. The result of this is plotted in Fig. 3. Three separate regions of lightning activity are observed: 1) $\Delta t < 0.01$s and $\Delta r < 10$ km, 2) $0.01\,\text{s} < \Delta t < 1\,\text{s}$ and $\Delta r < 15$ km, and 3) $\Delta t > 1$ s. In general, lightning activity belonging to group 1 corresponds to groups of CC discharges (Ballarotti et al. 2005); group 2, flashes with multiple CG discharges; and group 3, separate flashes. Hence, signals with $\Delta t > 1$ s or $\Delta r > 15$ km originate from a different flash. Vice versa, an individual stroke belongs to a particular flash if $\Delta t < 1$ s and $\Delta r < 15$ km. In addition, a temporal interstroke criterion $\Delta t_{\text{interstroke}} < 0.5$ s and a maximum multiplicity of 15 CG strokes per flash are used as well. If at least one signal in a flash is classified as CG, then we classify the flash as a CG flash, else it is classified as a CC flash. The position and peak current of the first return stroke are chosen as the position and peak current of the CG flash. In case of a CC flash, the mean of the different source point positions is used as the location of the CC flash.

Strokes and flashes are compared using the relative detection efficiency (RDE) concept to evaluate the relative performance of two different datasets by calculating

TABLE 1. Number of detections over research area 1 during May–September 2011 and 2012.

	Strokes	Flashes
MTRG	205 024	114 092
SAFIR	250 856	140 646
ATDnet	369 628	264 462
MTRG$^+$	393 636	217 020

the number of overlapping events registered by one system assuming the other as the truth, and vice versa. Consider two LLS A and B, with n_A and n_B as the number of detections by A and B, respectively; and $n_{A\cap B}$ as the number of detections simultaneously observed by both systems. Then, RDE(A out of B) = $n_{A\cap B}/n_B$. The latter was derived theoretically by Rubinstein (1992), and underlined its validity in the absence of any bias in the detection process. Hence, since LLS tend to locate more easily strokes with higher peak currents, the RDE values presented in this study likely overestimate the true value.

A stroke (flash) is considered the same in two datasets when $\Delta t \leq 1$ ms (1 s) and $\Delta r \leq 15$ km. The longer adopted time window for flashes is inherent to the duration of a flash, being a combination of different strokes. Following the argumentation in Drüe et al. (2007), the use of identical Δr and Δt thresholds, as applied to group strokes into flashes, is justified to determine whether a flash is detected by two networks. This is because Δr is chosen to assure that any signal that is part of the same flash falls within this radius. Hence, the position reported by one system would still be located inside Δr of the position reported by the other system, even if both systems use different single-point signals inside the same flash to reference the flash position. Vice versa, an overlap of two Δr areas and hence a possible wrong association of separated flashes can be excluded since the autocorrelation analysis (Fig. 3) did not reveal single-point signals between 15 km $< \Delta r <$ 50 km and $\Delta t <$ 1 s. A similar argument can be applied for Δt.

In section 4, the region of interest, "area 1," is restricted to latitude 49°–52°N and longitude 2°–7°E. This is an area of common overlap between the lightning networks described in section 2. To intercompare MTRG and ATDnet over a larger region, in "area 2" the boundaries are enlarged in section 5 to latitude 42°–53°N and longitude 5°W–9°E. The performance of the networks within these predefined boundaries is considered to be optimal to allow a proper intercomparison. The remaining figures in the text display the results regarding the flash analysis. As for strokes, results thereof are in addition to the flash analysis presented in the tables (except for Table 3).

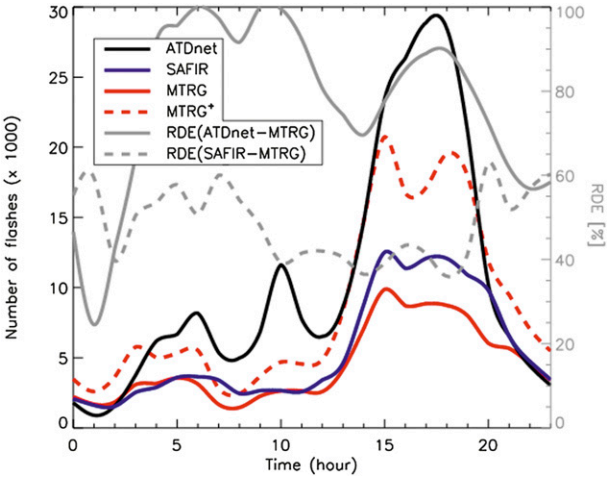

FIG. 4. Temporal distribution of the number of flashes detected by ATDnet (black), SAFIR (blue), MTRG (red/solid), and MTRG$^+$ (red/dashed) over research area 1 during May–September 2011 and 2012. In addition, the variation of the flash RDE (%) of ATDnet (gray/solid) and SAFIR (gray/dashed) with respect to MTRG is plotted as well.

4. Data comparison: Research area 1

a. Temporal and spatial distribution

Table 1 lists the total number of strokes and resulting flashes for each network over the period May–September 2011 and 2012. ATDnet detects more than SAFIR and MTRG, whereas MTRG$^+$ detects a similar quantity as ATDnet. A closer look at the diurnal temporal distributions of flashes detected by the individual networks, as plotted in Fig. 4, reveals that ATDnet outnumbers by far the detections of the other networks between 0300 and 2000 UTC, but is not the case at night. The latter can be partly understood, since the propagation of VLF follows the earth–ionospheric waveguide. Hence, the diurnal variability of the height of the ionosphere introduces significant degradations in ATDnet's performance (Lynn 1977; Gaffard et al. 2008). However, the reduction of ATDnet detection efficiency at night relative to during the day over Europe is primarily attributed to the interference between the sky wave propagation modes, introducing waveform deformations (Bennett et al. 2011). Additionally, one notices that the temporal distribution of MTRG$^+$ more closely follows the temporal behavior of ATDnet than MTRG. This could be an indication that a certain fraction of large amplitude CC discharges emitting sufficient VLF radiation are being picked up by ATDnet as well. This will be further discussed in section 4c.

Figure 5 plots flash density maps for MTRG, MTRG$^+$, SAFIR, and ATDnet using the method described in

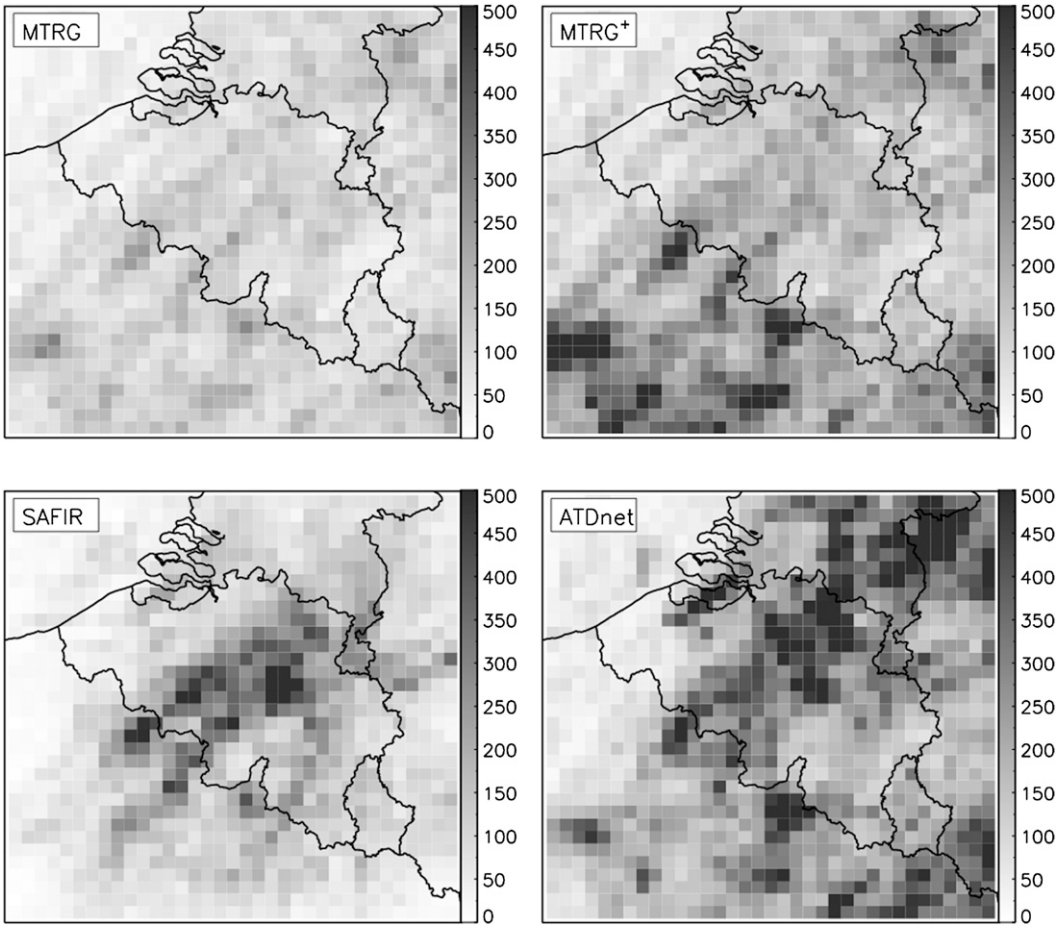

FIG. 5. Spatial distribution of the number of flashes detected by MTRG, MTRG$^+$, SAFIR, and ATDnet over research area 1 during May–September 2011 and 2012. Color shading indicates the absolute number of flashes per 10 $\times$ 10 km^2. Note that all values above 500 are given the same shade.

section 3. Some differences are noticeable between these networks. It is seen that 1) in general, the spatial distribution differs among the networks; 2) detections by SAFIR seem to be biased toward the center of Belgium, probably because of an inhomogeneous detection efficiency, favoring detections over the domain within the four SAFIR sensors; and 3) detections by MTRG are more or less homogeneous. The increased density in the center of Belgium, as seen by SAFIR and ATDnet, is not being picked up by MTRG.

One could wonder what causes ATDnet to detect much more compared to, for example, MTRG, resulting in an apparent different spatial behavior. First and foremost, note that the applied quality control settings within the individual central processors differ, whereby ATDnet accepts lightning detections with location errors a few factors larger than is allowed by MTRG. Second, a closer look into the raw sensor data of MTRG reveals that during a few days of severe thunderstorm activity during the 2011 storm season, several LS sensors were out of order for a short or longer time span around Belgium. Hence, because of these sensor outages, the performance of MTRG can be considered as substandard during the latter season. In addition, looking at the individual density maps for 2011 and 2012 (not shown here), the 2011 storm season dominates the total flash density map as presented in Fig. 5. It is thus likely that a combination of 1) applied quality control parameters, 2) sensor outages by MTRG, and 3) CC signals being picked up by ATDnet can explain the observed differences between ATDnet and the other networks over this particular region and period.

b. Spatial and temporal deviations

Median spatial deviations for correlated strokes and flashes between the different networks are given in Table 2. It is found that MTRG and ATDnet position overlapping detections closest to each other. The largest

TABLE 2. Relative detection efficiency and spatial deviation values belonging to research area 1.

	Stroke RDE (%)	Flash RDE (%)		Stroke RDE (%)	Flash RDE (%)	Median stroke deviation (km)	Median flash deviation (km)
MTRG out of SAFIR	28	37	SAFIR out of MTRG	34	46	6.5	7.1
MTRG out of ATDnet	26	34	ATDnet out of MTRG	47	80	1.9	2.8
ATDnet out of SAFIR	27	60	SAFIR out of ATDnet	18	32	6.7	7.5
$MTRG^+$ out of ATDnet	40	57	ATDnet out of $MTRG^+$	39	69	2.0	3.0

deviations are found when comparing SAFIR to the other networks. This behavior is visualized in Fig. 6, plotting the spatial offsets between overlapping flashes. The flashes are grouped more closely around the (0, 0) point for MTRG–ATDnet, whereas the deviations are more spread out when compared against SAFIR. In addition, we overlay the cumulative fraction of the distance between overlapping flashes. Besides the median deviation values in Table 2, we deduce that, for example, 80% of the distance between overlapping flashes have a spatial difference that falls within 7.2, 11.1, and 11.5 km for MTRG–ATDnet, SAFIR–MTRG, and SAFIR–ATDnet, respectively.

Figure 7 plots the distribution of the time differences between correlated flashes. It is observed that the median time difference between SAFIR–ATDnet, MTRG–SAFIR, MTRG–ATDnet is −120, 25, and −100 μs, respectively. The standard deviation in all cases is ~100 μs. Similar values are found at the level of strokes.

c. *Relative detection efficiency*

RDE values are listed in Table 2. It is seen that 1) the lowest overall RDE values are found when comparing either ATDnet or MTRG against SAFIR. This is not surprising since the median LA of SAFIR is ~6 km, based on ground-truth observations (Poelman et al. 2013), diminishing the number of overlaps. 2) In general, the highest RDE values are found between MTRG and ATDnet with, for instance, 80% of ATDnet's flashes overlapping MTRG flashes. 3) We find that MTRG recognizes 34% of the flashes out of ATDnet. This value increases to 57% when considering $MTRG^+$ out of ATDnet. Thus, about 25% of the CC flashes detected by $MTRG^+$ have an overlap with ATDnet. In other words, CC flashes make up the lower limit of ~25% of ATDnet's flashes, assuming a correct discrimination between CG and CG lightning in the $MTRG^+$ dataset. The value of this lower limit decreases to about 15% when strokes are considered.

In addition to the temporal distribution, we plot in Fig. 4 the variation of the relative flash detection efficiency of ATDnet and SAFIR out of MTRG as a function of time of day. One observes that for SAFIR, the RDE varies continuously with no clear trend during the course of the entire 24 h, whereas clearly the RDE for ATDnet is high during the day and drops at night.

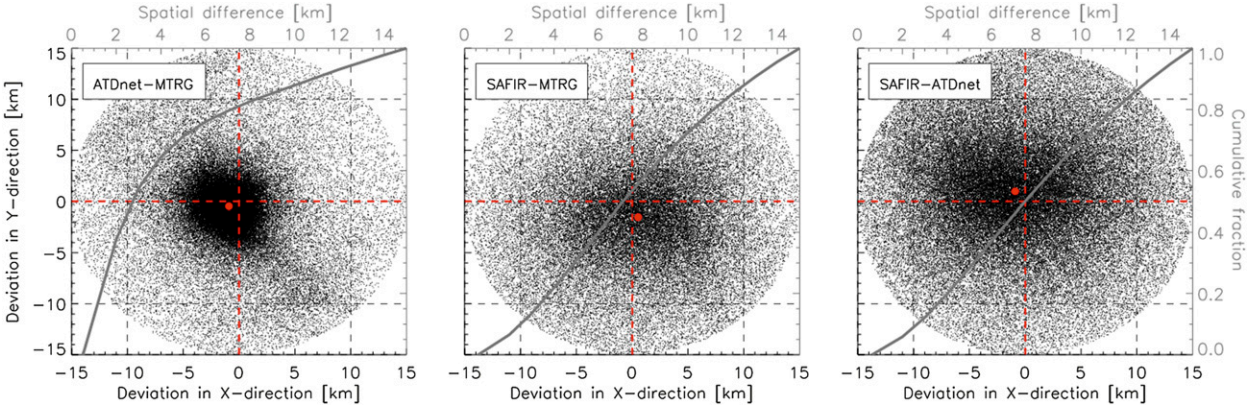

FIG. 6. Spatial deviations are plotted between corresponding flashes in the cases of (left) ATDnet–MTRG, (middle) SAFIR–MTRG, and (right) SAFIR–ATDnet over research area 1. Red dot indicates the median offset from the origin (0, 0). In addition, the cumulative fraction of the distance between correlating flashes is overplotted (gray).

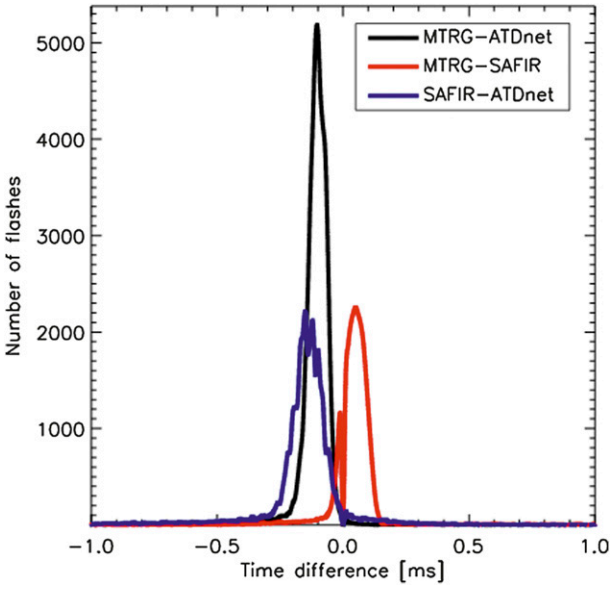

FIG. 7. Distribution of the time difference between corresponding flashes in the cases of MTRG–ATDnet (black), MTRG–SAFIR (red), and SAFIR–ATDnet (blue). Data are grouped into 0.01-ms bin sizes.

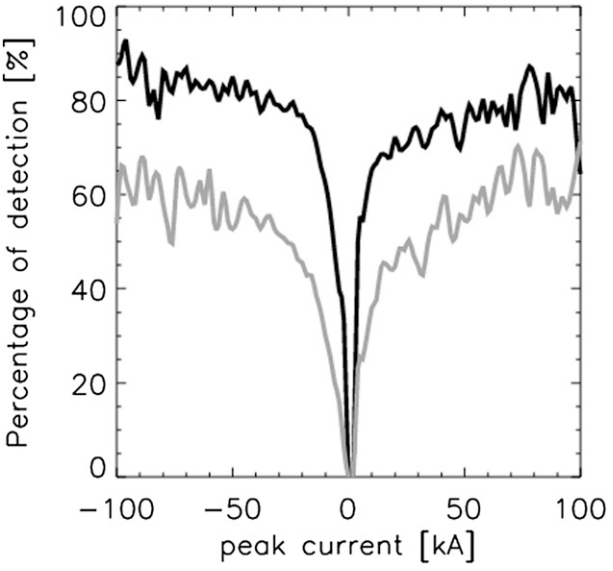

FIG. 8. Percentage of detection of ATDnet (black) and SAFIR (gray) flashes out of MTRG flashes as a function of peak current, adopting a bin size of 2 kA.

Figure 8 plots the flash RDE of ATDnet and SAFIR out of MTRG as a function of MTRG flash peak current. Note that the observed large variations at high negative and positive peak currents are due to the low number of events. In general we find that RDE drops with decreasing peak current and increases for flashes with higher peak currents. This behavior is expected, since radiation from lightning discharges with higher peak currents tend to be easier picked up and better located by the sensors in a network.

d. Capturing the spatial distribution of thunderstorms

In this section, we determine the capability of a network to capture the spatial distribution of storm events on a daily basis during May–September 2011 and 2012. As an example, we plot the spatial flash distribution on 28 June 2011 in Fig. 9, color coded as a function of time. At first glance, the spatial and temporal patterns agree well among the networks. On the other hand, it appears that flashes belonging to some particular cells are grouped tighter in MTRG and ATDnet opposed to SAFIR.

To measure the ability of a network to correctly detect the extent of thunderstorms, we follow the approach as presented in Lagouvardos et al. (2009). First, we divide the area in grid boxes of $10 \times 10\,\mathrm{km}^2$. Second, we construct a 2×2 contingency table, assuming one network as ''ground truth,'' against which another network is validated and apply this to each storm day. The values in

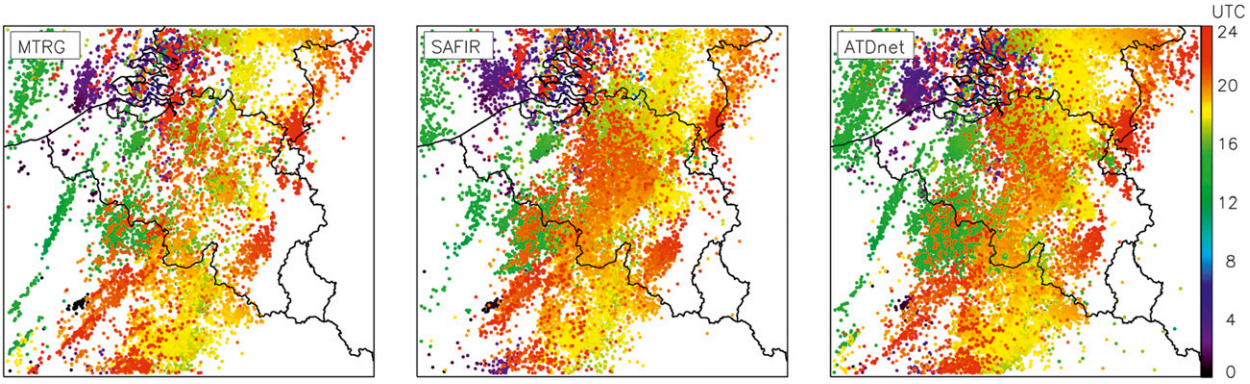

FIG. 9. Temporal and spatial evolution of the detected flashes on 28 Jun 2011 by (left) MTRG, (middle) SAFIR, and (right) ATDnet over research area 1.

TABLE 3. POD, FAR, and PC values belonging to area 1 during May–September 2011 and 2012.

Validation/ground truth	POD	FAR	PC
SAFIR/MTRG	0.90	0.14	0.79
SAFIR/ATDnet	0.83	0.10	0.76
MTRG/SAFIR	0.86	0.10	0.79
MTRG/ATDnet	0.83	0.05	0.79
ATDnet/SAFIR	0.90	0.17	0.76
ATDnet/MTRG	0.95	0.17	0.79

the contingency table are as follows: A, the number of grid boxes for which both networks observe at least one flash (=hits); B, the number of grid boxes for which the ground-truth dataset did not detect any flash but the validation network did (=false alarm); C, the number of grid boxes for which the ground-truth dataset detects at least one flash but the validation network not (=misses); and D, the number of grid boxes where neither the ground-truth dataset nor the validation dataset detect any flash (=correct negatives). It follows that 1) the probability of detection (POD) equals $A/(A + C)$, with a preferred value as close to 1 as possible; 2) the false alarm ratio (FAR) is equal to $B/(A + B)$ and should be as small as possible; and 3) the proportion correct (PC) equals $(A + D)/(A + B + C + D)$. The resulting values for the period May–September 2011 and 2012 are listed in Table 3, with POD values ranging between 0.83 and 0.95, FAR between 0.05 and 0.17, and PC between 0.76 and 0.79. It is found that even though the RDE values of SAFIR against MTRG and/or ATDnet as presented in Table 2 are the lowest, the POD never drops below 0.83 and the maximum FAR is 0.17. Hence, we conclude that SAFIR is able to capture efficiently the areas affected by lightning, as is the case for MTRG and ATDnet. Thus, each network, unique in the choice of sensors and detection technology, is able to capture the electrical activity in thunderstorms.

5. Data comparison: Research area 2

In this section, we expand the region of interest to latitude 42°–53°N and longitude 5°W–9°E—an area covering Belgium, France, the Netherlands, southern England, western Germany, and northern Spain. In this way, potential local effects such as sensor outages are suppressed. Only MTRG, MTRG$^+$, and ATDnet are considered, as the Belgian SAFIR network is not capable of detecting lightning activity over this larger area.

a. Temporal and spatial distribution

Table 4 lists the number of strokes and resulting flashes for ATDnet, MTRG, and MTRG$^+$. The distribution of

TABLE 4. Number of detections over research area 2 during May–September 2011 and 2012.

	Strokes	Flashes
MTRG	2 317 648	1 205 134
ATDnet	3 377 845	2 403 434
MTRG$^+$	4 636 339	2 415 182

the number of detected flashes as a function of time for ATDnet, MTRG, and MTRG$^+$ is plotted in Fig. 10. As in section 4, it is seen that ATDnet detects more during the day compared to MTRG, while a drop is noticed at night. However, MTRG$^+$ now has roughly the same distribution as ATDnet during the day.

Flash density maps for MTRG, MTRG$^+$, and ATDnet are presented in Fig. 11. It is seen that MTRG follows the same pattern as ATDnet, albeit with a lower detection rate. On the other hand, MTRG$^+$ detections are more densely spaced around the southwest of France and around the Paris region compared to MTRG. To quantify the ability of MTRG$^+$ to detect CC activity, the spatial distribution of the CC/CG flash ratio is presented as well in Fig. 11. It is seen that this ratio increases to values between 2 and 4 mainly in the southwest of France and the region around Paris. This is not surprising, since short baselines between LS sensors at these particular regions lead to a better detection efficiency for intracloud lightning.

b. Relative detection efficiency and spatial deviation

RDE values for strokes and flashes are listed in Table 5, together with the median spatial deviation between

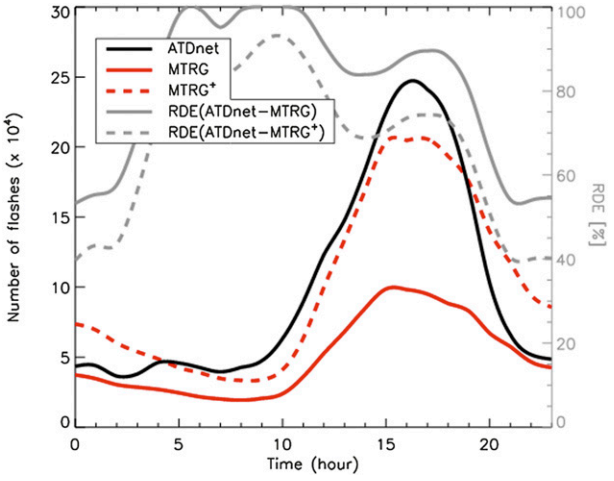

FIG. 10. Temporal distribution of the number of flashes detected over research area 2 during May–September 2011 and 2012 by ATDnet (black), MTRG (red, solid), and MTRG$^+$ (red, dashed). In addition, the RDE (%) of ATDnet w.r.t. MTRG (gray/solid) and MTRG$^+$ (gray/dashed) is plotted as a function of time.

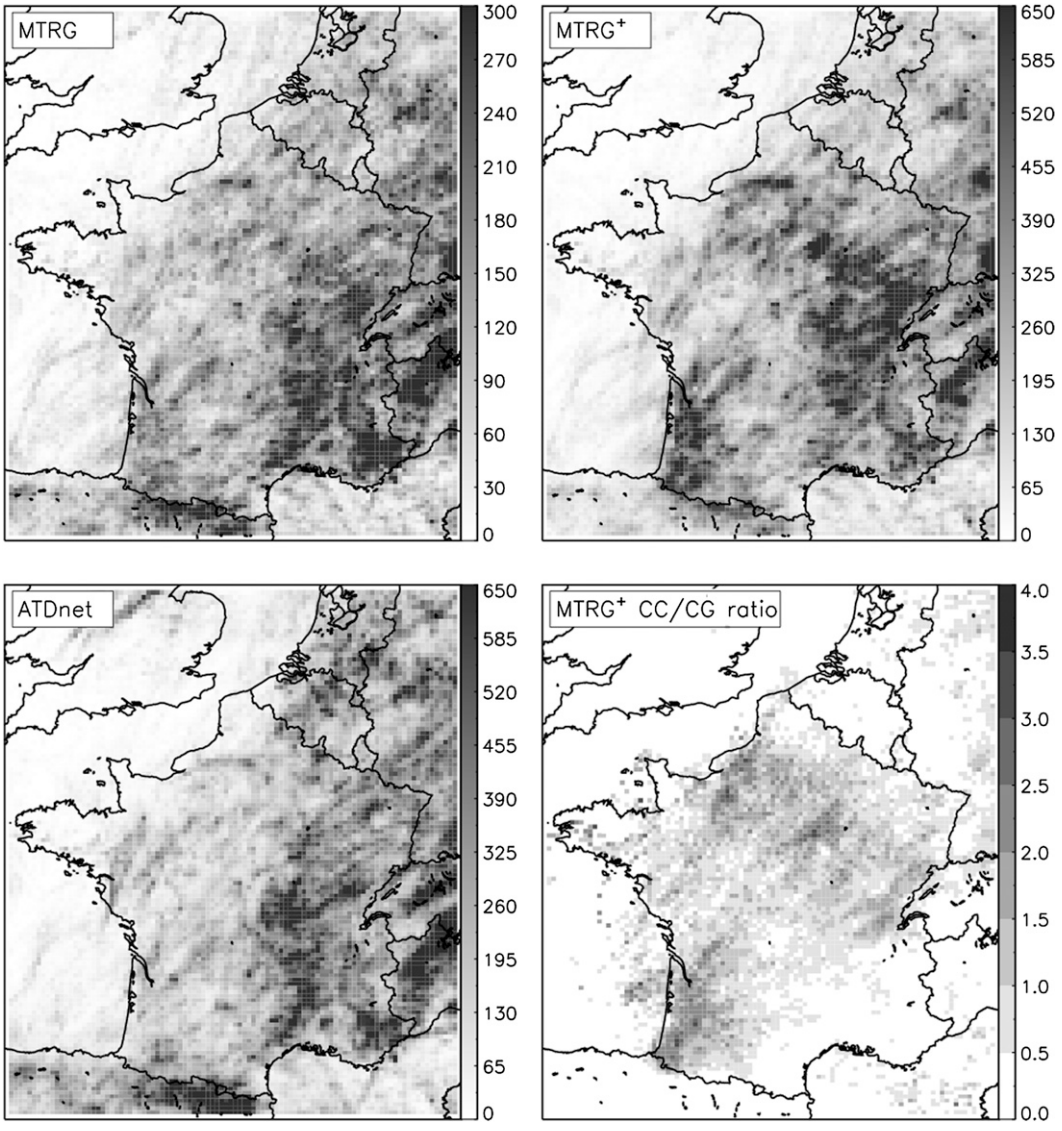

FIG. 11. Spatial distribution of the number of flashes detected by MTRG, MTRG$^+$, and ATDnet over research area 2 during May–September 2011 and 2012. Color shading indicates the absolute number of flashes per $10 \times 10\,\text{km}^2$. Note the different gray scales in the plots. In addition, the CC/CG flash ratio of MTRG$^+$ is plotted as well.

overlapping strokes and flashes. First, median spatial deviation values are comparable to the values found in section 4. Second, MTRG recognizes 40% of ATDnet's flashes. This value increases to 66%, when comparing MTRG$^+$ out of ATDnet. This indicates that a certain fraction of CC signals are being picked up by ATDnet, assuming a correct discrimination by MTRG$^+$, and is similar to the value found over research area 1 (section 4). Hence, we conclude that the majority of the flashes detected by ATDnet are CG flashes, mixed with a lower limit of ~25% CC flashes. On the stroke level, it is found that 18% of ATDnet's strokes are of type intracloud following a similar reasoning in the case of flashes—a value comparable to the 26% found comparing WWLLN strokes to the Los Alamos Sferic Array in Florida (Jacobson et al. 2006).

In addition to the temporal distributions in Fig. 10, we plot the variation of the RDE of ATDnet out of MTRG and MTRG$^+$. Again, the RDE is high during the day and drops at night—similar to the trend observed over area 1.

6. Summary and discussion

In this paper three distinct lightning location systems covering Belgium during two storm seasons between

TABLE 5. Relative detection efficiency and spatial deviation values belonging to research area 2.

	Stroke RDE (%)	Flash RDE (%)		Stroke RDE (%)	Flash RDE (%)	Median stroke deviation (km)	Median flash deviation (km)
MTRG out of ATDnet	33	40	ATDnet out of MTRG	49	80	1.9	2.7
$MTRG^+$ out of ATDnet	51	66	ATDnet out of $MTRG^+$	37	66	1.9	2.8

May and September during both 2011 and 2012 are compared. Two research areas, different in size, are chosen to investigate the spatial and temporal variations. Sensor configuration, type of sensors used, and the applied technology and quality control settings to process the data give rise to a variation in the number and location of detected lightning signals.

We find that ATDnet detects more lightning signals compared to the CG datasets of MTRG and SAFIR. However, $MTRG^+$, containing the total lightning detections by MTRG, follows more closely the temporal distribution of ATDnet. Whereas for SAFIR, MTRG, and $MTRG^+$ a value of ~1.8 for the stroke/flash ratio is found, this decreases to 1.4 in case of ATDnet for areas 1 and 2; see Tables 1 and 4. As such, the flash algorithm applied to the different datasets seems to be less effective in grouping strokes for ATDnet than is the case for the other networks. A potential explanation is that ATDnet is more likely to detect the first—and most likely strongest—stroke in a flash, but it is less likely to detect subsequent return strokes (see Poelman et al. 2013). Further investigation is needed, but it has been out of the scope for this study.

For the first time, an attempt has been made to quantify the fraction of CC signals that are being picked up by ATDnet. A lower limit of ~25% is found when flashes are considered. ATDnet's relative detection efficiency peaks during the day and exhibits a nocturnal drop. This is attributed to modal interferences and the increase of the effective ionospheric height due to a reduction in photoionization from solar UV radiation. Nevertheless, when compared to MTRG we find a median spatial flash deviation of about 3 km and high RDE values. Furthermore, storm-scale POD values of ~80% and 90% and low FAR values are found for ATDnet and MTRG, respectively, demonstrating the capability to map electrical activity within thunderstorms.

A median spatial flash deviation of about 7 km of SAFIR referenced against MTRG and ATDnet is found. This is a factor of about 2 larger than what is found between MTRG and ATDnet. RDE values are lower compared to the ones between MTRG and ATDnet and could be due to the reduced LA of SAFIR. Opposed to ATDnet, the temporal RDE variations do not favor a specific moment during the day. The POD and FAR values reveal that SAFIR is capable of capturing the majority of lightning activity in storm cells.

Acknowledgments. DRP is grateful for the support provided by the Belgian Science Policy Office (BELSPO), through research project MINMETEO. The authors thank Wolfgang Schulz from OVE-ALDIS; Dirk Klugmann, Melanie Collins, and Greg Callaghan from UKMO; and Laurent Delobbe from RMIB for the useful discussions related to this paper. The authors are grateful to the referees for their constructive comments, which improved the content and presentation considerably.

REFERENCES

Abreu, D., D. Chandan, R. H. Holzworth, and K. Strong, 2010: A performance assessment of the World Wide Lightning Location Network (WWLLN) via comparison with the Canadian Lightning Detection Network (CLDN). *Atmos. Meas. Tech. Discuss.,* **3,** 1861–1887, doi:10.5194/amtd-3-1861-2010.

Ballarotti, M. G., M. M. F. Saba, and O. Pinto Jr., 2005: High-speed camera observations of negative ground flashes on a millisecond-scale. *Geophys. Res. Lett.,* **32,** L23082, doi:10.1029/2005GL023889.

Bennett, A. J., G. Callaghan, C. Gaffard, J. Nash, and R. Smout, 2010: The effect of changes in lightning waveform propagation characteristics on the UK Met Office long range lightning location network (ATDnet). *Proc. 21st Int. Lightning Detection Conf.,* Orlando, FL, Vaisala, 13 pp. [Available online at http://www.vaisala.com/en/events/ildcilmc/Pages/ILDC-2010-Archive.aspx.]

——, C. Gaffard, J. Nash, G. Callaghan, and N. C. Atkinson, 2011: The effect of modal interference on VLF long-range lightning location networks using the waveform correlation technique. *J. Atmos. Oceanic Technol.,* **28,** 993–1006.

Biagi, C. J., K. L. Cummins, K. E. Kehoe, and E. P. Krider, 2007: National Lightning Detection Network (NLDN) performance in southern Arizona, Texas, and Oklahoma in 2003–2004. *J. Geophys. Res.,* **112,** D05208, doi:10.1029/2006JD007341.

Boccippio, D. J., and Coauthors, 2000: The Optical Transient Detector (OTD): Instrument characteristics and cross-sensor validation. *J. Atmos. Oceanic Technol.,* **17,** 441–458.

Cummins, K. L., M. J. Murphy, E. A. Bardo, W. L. Hiscox, R. B. Pyle, and A. E. Pifer, 1998: A combined TOA/MDF technology upgrade of the U.S. National Lightning Detection Network. *J. Geophys. Res.,* **103** (D8), 9035–9044.

——, J. A. Cramer, C. Biagi, E. P. Krider, J. Jerauld, M. A. Uman, and V. A. Rakov, 2006: The U.S. National Lightning Detection Network: Post-upgrade status. Preprints, *Second Conf.*

on Meteorological Applications of Lightning Data, Atlanta, GA, Amer. Meteor. Soc., 6.1. [Available online at https://ams.confex.com/ams/Annual2006/techprogram/paper_105142.htm.]

——, A. E. Pifer, M. Pezze, T. Rogers, N. Honma, and M. Tatsumi, 2011: Improved detection of winter lightning in the Tohoku region of Japan using Vaisala's LS700x technology. *Proc. Third Int. Symp. on Winter Lightning,* Sapporo, Japan, ISWL, 6 pp.

Diendorfer, G., 2010: LLS performance validation using lightning to towers. *Proc. 21st Int. Lightning Detection Conf.,* Orlando, FL, Vaisala, 15 pp. [Available online at http://www.vaisala.com/en/events/ildcilmc/Pages/ILDC-2010-Archive.aspx.]

Drüe, C., T. Hauf, U. Finke, S. Keyn, and O. Kreyer, 2007: Comparison of a SAFIR lightning detection network in northern Germany to the operational BLIDS network. *J. Geophys. Res.,* **112,** D18114, doi:10.1029/2006JD007680.

Finke, U., 1999: Space–time correlations of lightning distributions. *Mon. Wea. Rev.,* **127,** 1850–1861.

Gaffard, C., and Coauthors, 2008: Observing lightning around the globe from the surface. *Proc. 20th Int. Lightning Detection Conf.,* Tucson, AZ, Vaisala, 12 pp. [Available online at http://www.vaisala.com/en/events/ildcilmc/Pages/ILDC-2008-Archive.aspx.]

Grant, M. D., K. J. Nixon, and I. R. Jandrell, 2012: Positive polarity: Misclassification between intracloud and cloud-to-ground discharges in the Southern African Lightning Detection Network. *Proc. 22nd Int. Lightning Detection Conf.,* Broomfield, CO, Vaisala, 5 pp. [Available online at http://www.vaisala.com/en/events/ildcilmc/Pages/ILDC-2012-archive.aspx.]

Honma, H., K. L. Cummins, M. J. Murphy, A. E. Pifer, and T. Rogers, 2011: Improved lightning locations in the Tokohu region of Japan using propagation and waveform onset corrections. *Proc. Third Int. Symp. on Winter Lightning,* Sapporo, Japan, ISWL, 6 pp.

Jacobson, A. R., R. Holzworth, J. Harlin, R. Dowden, and E. Lay, 2006: Performance assessment of the World Wide Lightning Location Network (WWLLN), using the Los Alamos Sferic Array (LASA) as ground truth. *J. Atmos. Oceanic Technol.,* **23,** 1082–1092.

Jerauld, J., V. A. Rakov, M. A. Uman, K. J. Rambo, D. M. Jordan, K. L. Cummins, and J. A. Cramer, 2005: An evaluation of the performance characteristics of the U.S. National Lightning Detection Network in Florida using rocket-triggered lightning. *J. Geophys. Res.,* **110,** D19106, doi:10.1029/2005JD005924.

Keogh, S. J., E. Hibbett, J. Nash, and J. Eyre, 2006: The Met Office Arrival Time Difference (ATD) system for thunderstorms detection and lightning location. Forecasting Research Tech. Rep. 488, 22 pp.

Kohn, M., E. Galanti, C. Price, K. Lagouvardos, and V. Kotroni, 2011: Nowcasting thunderstorms in the Mediterranean region using lightning data. *Atmos. Res.,* **100,** 489–502.

Kotroni, V., and K. Lagouvardos, 2008: Lightning occurrence in relation with elevation, terrain slope, and vegetation cover in the Mediterranean. *J. Geophys. Res.,* **113,** D21118, doi:10.1029/2008JD010605.

Kuk, B. J., H. I. Kim, J. S. Ha, and H. K. Lee, 2011: Intercomparison study of cloud-to-ground lightning flashes observed by KARITLDS and KLDN at South Korea. *J. Appl. Meteor. Climatol.,* **50,** 224–232.

Lagouvardos, K., V. Kotroni, H.-D. Betz, and K. Schmidt, 2009: A comparison of lightning data provided by ZEUS and LINET networks over western Europe. *Nat. Hazards Earth Syst. Sci.,* **9,** 1713–1717, doi:10.5194/nhess-9-1713-2009.

Lynn, K. J. W., 1977: VLF modal interference over west-east paths. *J. Atmos. Terr. Phys.,* **39,** 347–357.

Nag, A., and Coauthors, 2011: Evaluation of U.S. National Lightning Detection Network performance characteristics using rocket-triggered lightning data acquired in 2004–2009. *J. Geophys. Res.,* **116,** D02123, doi:10.1029/2010JD014929.

Orville, R., G. Huffines, W. Burrows, R. Holle, and K. Cummins, 2002: The North American Lightning Detection Network (NLDN)—First results: 1998–2000. *Mon. Wea. Rev.,* **130,** 2098–2108.

Poelman, D. R., W. Schulz, and C. Vergeiner, 2013: Performance characteristics of three distinct lightning detection networks covering Belgium. *J. Atmos. Oceanic Technol.,* **30,** 942–951.

Rodger, C. J., S. Werner, J. B. Brundell, E. H. Lay, N. R. Thomson, R. H. Holzworth, and R. L. Dowden, 2006: Detection efficiency of the VLF World-Wide Lightning Location Network (WWLLN): Initial case study. *Ann. Geophys.,* **24,** 3197–3214, doi:10.5194/angeo-24-3197-2006.

Rubinstein, M., 1992: On the estimation of the detection efficiency by comparison of adjacent lightning location systems. *Proc. 22nd Int. Conf. on Lightning Protection,* Berlin, Germany, ICLP, 5 pp.

Schulz, W., H. Pichler, and G. Diendorfer, 2010: Evaluation of 45 negative flashes based on E-field measurements, video data and lightning location data in Austria. *Proc. 30th Int. Conf. on Lightning Protection,* Cagliari, Italy, ICLP, 1011-1–1011-4.

Thomas, R. J., P. R. Krehbiel, W. Rison, T. Hamlin, D. J. Boccippio, S. J. Goodman, and H. J. Christian, 2000: Comparison of ground-based 3-dimensional lightning mapping observations with satellite-based LIS observations in Oklahoma. *Geophys. Res. Lett.,* **27,** 1703–1706, doi:10.1029/1999GL010845.

Wacker, R. and R. Orville, 1999a: Changes in measured lightning flash count and return stroke peak current after the 1994 U.S. National Lightning Detection Network upgrade: 1. Observations. *J. Geophys. Res.,* **104** (D2), 2151–2157.

——, and ——, 1999b: Changes in measured lightning flash count and return stroke peak current after the 1994 U.S. National Lightning Detection Network Upgrade: 2. Theory. *J. Geophys. Res.,* **104** (D2), 2159–2162.